DOI: 10.1002/ange.201409314

Plasmonics

Shedding Light on the Extinction-Enhancement Duality in Gold Nanostar-Enhanced Raman Spectroscopy**

*Ming Li, Jeon Woong Kang, Ramachandra Rao Dasari, and Ishan Barman**

Abstract: *Surface-enhanced Raman spectroscopy (SERS) has evolved from an esoteric physical phenomenon to a robust and effective analytical method recently. The need of addressing both the field enhancement and the extinction of nanoparticle suspensions, however, has been underappreciated despite its substantive impact on the sensing performance. A systematic experimental investigation of SERS enhancement and attenuation is performed in suspensions of gold nanostars, which exhibit a markedly different behavior in relation to conventional nanoparticles. The relationship is elucidated between the SERS enhancement and the localized surface plasmon resonance band, and the effect of the concentration of the gold nanostars on the signal propagation is investigated. It is shown that an optimal concentration of gold nanostars exists to maximize the enhancement factor (EF), and the maximum EF occurs when the LSPR band is blue-shifted from the excitation wavelength rather than at the on-resonance position.*

Nanoparticle-enhanced Raman spectroscopy assays have recently been reported to exceed detection limits of fluorescence-based methods and conventional immunoassays while being quantitative over a wide range of probe concentrations.[1,2] Spurred by the explosion of research in plasmonics, surface-enhanced Raman spectroscopy (SERS) has matured from an interesting laboratory phenomenon plagued by irreproducibility concerns to a robust and effective analytical tool offering high sensitivity and chemical specificity (and therefore extensive multiplexing capability) as well as stable signals and surface selectivity.[3–8] Meeting these specifications simultaneously, however, has been a major experimental challenge reaffirming the need for methodical investigation of the nanoscale metal structures that control and tune the enhancement of the SERS signal.

Significant effort has been directed toward understanding the underlying mechanisms of SERS and exploiting them to obtain the largest enhancement factors (EFs) possible while concomitantly controlling variability in their spectral response.[9] Given the dominant nature and clearer understanding of electromagnetic (EM) enhancement, the principal design goal in construction of high-performance SERS sensing platforms[10,11] has been to reliably control the geometry and composition of the metal nanostructures, which influence the localized surface plasmon resonance (LSPR) properties.[12] Recent advances in colloidal synthesis and nanofabrication techniques have enabled the tailoring of such nanostructures with desirable morphology and thereby tunable plasmonic properties.[13,14] In particular, experiments backed by theoretical simulations have shown that anisotropic structures can concentrate the electric field around the sharp tips ("hot spots") because of the lightning rod effect.[15,16] These hot spots dominate the SERS enhancement as evidenced by the significantly higher EFs of gold nanostars in comparison to spherical nanoparticles and nanorods.[16] Importantly, by modulating the protrusion length and density as well as the core size, the LSPR band of gold nanostars can be easily tuned to the near-infrared (NIR) spectral region, which is a preferable window (700–1100 nm) for investigations in biological tissue matrices with little light scattering, absorption, and fluorescence.[17,18]

Despite the promising performance of these nanostars in the detection of circulating biomarkers in human serum samples,[7,16,19,20] these preliminary studies have brought to light specific scientific questions. Critically, there is a lack of understanding of the behavior of gold nanoparticles dispersed throughout the biological fluid or tissue matrix, which stems from the often overlooked competition between the field enhancement and extinction in the nanostar colloids. While a few studies have touched on the interplay of absorption and scattering on SERS signal propagation,[21] it is only recently that the link between the SERS enhancement and the extinction of both the incident and scattered light during propagation has been recognized for spherical constructs.[22]

In this work, we seek to optimize the gold nanostar to obtain the maximum SERS enhancement and to directly probe the competition of SERS enhancement and attenuation in their suspensions. These two interconnected foci provide the first systematic investigation of plasmonic tunability of the nanostars and the resultant effect on SERS enhancement and propagation processes. Here, using a gold-seed-mediated

[*] Dr. M. Li, Dr. J. W. Kang, Dr. R. R. Dasari
Laser Biomedical Research Center
George R. Harrison Spectroscopy Laboratory
Massachusetts Institute of Technology
Cambridge, MA 02139 (USA)
Dr. M. Li, Prof. I. Barman
Departments of Mechanical and Biomedical Engineering
Johns Hopkins University, Baltimore, MD 21218 (USA)
Prof. I. Barman
Department of Oncology, Johns Hopkins University
Baltimore, MD 21287 (USA)
E-mail: ibarman@jhu.edu
Homepage: https://engineering.jhu.edu/barman/

[**] This research was supported by the JHU Whiting School of Engineering Startup Funds, NIH NIBIB (grant number 9P41EB015871-27) and the MIT SkolTech initiative. This work made use of the MRSEC shared experimental facilities at MIT, supported by the National Science Foundation under award number DMR-08-19762.

Supporting information for this article is available on the WWW under http://dx.doi.org/10.1002/anie.201409314.

approach, we tune the LSPR band of gold nanostars from the visible to the NIR region and further investigate the effect of LSPR band on the SERS enhancement. Additionally, we experimentally determine the existence of an optimal concentration of nanostars in suspension, which suitably balances the propagation of incident and Raman-scattered light and the near-field SERS enhancement.

A series of gold nanostars were prepared by changing the gold seed concentration to tailor the plasmonic nanoarchitecture (detailed in the Supporting Information). Briefly, different amounts of polyvinylpyrrolidone (PVP)-coated gold seed solutions were added to a 10 mM PVP DMF solution with the addition of 82 μL 50 mM $HAuCl_4{\cdot}x\,H_2O$ aqueous solution, followed by centrifugation and washing after 3 h growth at room temperature. Figure 1 shows the morphological evolution of the synthesized gold nanostars as characterized by TEM. These representative TEM images illustrate the influence of the gold seed concentration on the resultant core size as well as the length and density of protrusions.

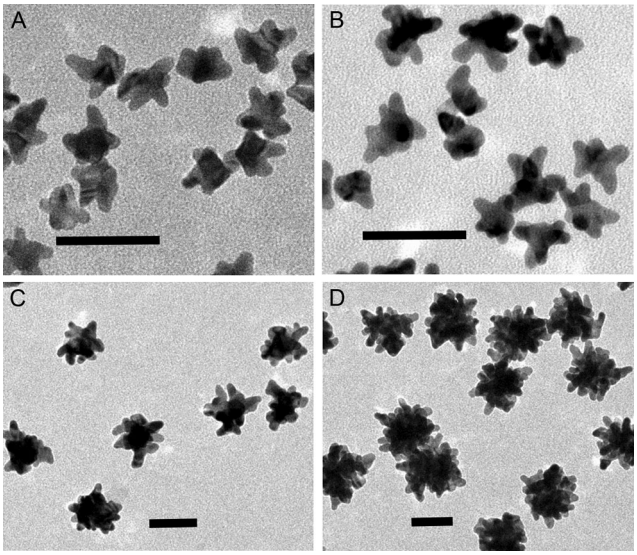

Figure 1. Representative TEM images of gold nanostars synthesized at different gold seed concentrations by the seed-mediated method. The relative concentration of the gold seed solution was: A) 16.6, B) 12.5, C) 1.66, and D) 0.36 pM. (scale bar: 50 nm).

The specific modulation of the gold nanostar geometry facilitated tunable LSPR band from the visible to the NIR. Figure 2 A displays optical images of gold seed and nanostar suspensions synthesized at different gold seed concentrations in range of vibrant colors from purple to gray and blue. As the excitation of a LSPR mode maximizes the interaction with the incident field, characteristic features are generated in the optical response, notably peaks in the optical extinction spectrum. This explains the characteristic transmission colors observed in Figure 2 A. The extinction spectra of the colloidal suspensions of these gold nanostars were measured (Figure 2 B). Expectedly, we observe significant red-shift in the LSPR wavelength with the decrease of the seed concentration. This facile route of tailoring the LSPR band from about

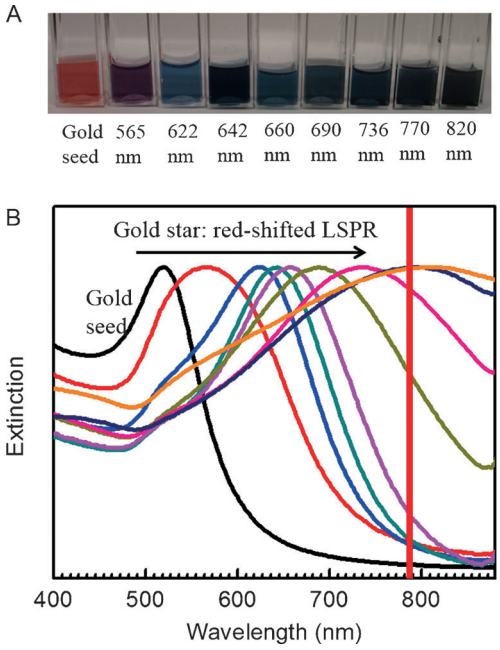

Figure 2. Optical images and extinction spectra of various gold nanostar suspensions. A) Optical images of gold seed and nanostar suspensions prepared by modulating the gold seed concentration. Left to right: gold seed, 565, 622, 642, 660, 690, 736, 770, and 820 nm LSPR bands. B) Extinction spectra of corresponding colloidal suspensions. The red line indicates the 785 laser excitation wavelength used in this study.

565 to 820 nm ensures the necessary flexibility for probing in the NIR diagnostic window.

We first examined the optical extinction of the incident light as it propagates through the gold nanostar suspension (Figure 3 A,B). The gold nanostar with the LSPR band of 736 nm is used here. The incident laser intensity gradually decreases as it propagates deeper in the gold nanostar suspension. Also, a higher concentration of gold nanostar in the suspension displays larger attenuation of the propagating beam. In particular, we see that the suspension of the 4 pM gold nanostar suspension has a much bigger penetration depth, and the light attenuates slowly in comparison to the 20 pM gold nanostar suspension (Figure 3 A).

A more quantitative measure of the optical extinction of the gold nanostar suspension as a function of the penetration depth is provided in Figure 3 B. The attenuation of light through the nanostar suspension is in agreement with Beer–Lambert estimates, which posits that the extinction of the incident light can be described as $I(d) = I(0)e^{-dn\rho C_{ext}}$, where I is the light intensity, d the propagation distance, n the effective refractive index, ρ the number of gold nanostar and C_{ext} the extinction cross-section of gold nanostar in the suspension. A similar, but not identical, impact of optical extinction is also perceived by the Raman-scattered light as it propagates to the collection optics. Additionally, since optical extinction shows considerable wavelength dependence mediated by the architecture of the nanostars, attenuation of different Raman peaks exhibits non-linearity with respect to concentration of nanoparticles. This phenomenon must be

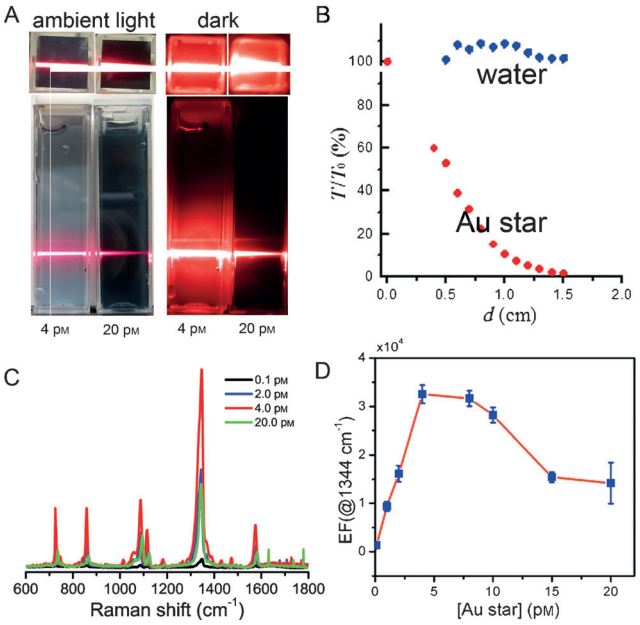

Figure 3. Optical extinction of the incident light in the gold nanostar suspension. A) Optical images demonstrating the extinction effect in suspensions. Optical images were taken for 4 pM and 20 pM gold nanostar suspensions both in ambient light and in the dark with 632.8 nm HeNe laser incidence, respectively. B) Optical extinction as a function of the propagation distance (d) in water and in the suspension of 4 pM gold nanostar under 632.8 nm HeNe laser incidence. C) Representative SERS spectra of 4-NTP in suspensions of various gold nanostar concentrations, and D) SERS EFs as a function of the gold nanostar concentration.

addressed to accurately relate the recorded signal to the analyte content.

Evidently, the optical extinction process acts against the SERS enhancement phenomenon as less Raman photons reach the detector. Therefore, one would expect a threshold concentration value that optimizes the trade-off between optical extinction and electromagnetic enhancement. Based on this conjecture, SERS at different gold nanostar concentrations was investigated using 0.5 μM non-fluorescent 4-nitrobenzenethiol (4-NTP) as the Raman reporter under laser excitation at 785 nm. Critically, 4-NTP has a strong affinity toward the gold surface because of the formation of a semi-covalent Au–S bond.[23,24] Table S1 lists the principal vibrational modes and their corresponding Raman shifts observed in the SERS spectra of 4-NTP molecules in the presence of the gold nanostar.

Figure 3C shows that the SERS intensity first increases and then decreases as the gold nanostar concentration increases. The SERS EFs as a function of the gold nanostar concentration are quantified in Figure 3D. Clearly, there exists an optimal concentration (4 pM) at which the EF has a maximum value (3.4×10^4) as a direct consequence of the competition between the enhancement and extinction phenomena. Whilst we appreciate that a direct one-to-one comparison is difficult, the ensemble-averaged EF obtained here compares favorably with previous studies employing gold nanostars and provides a tentative framework for the number of nanostars required for application in biological fluids. These findings imply that in developing practical assays for biomarkers in body fluids one would have to consider the extinction of the nanostars in context of their higher turbidity (absorption and scattering) as well as alternate sample-holder designs possessing larger surface area for SERS probing but with shallower depths to reduce the extinction impact.

Additionally, the classical EM theory hypothesizes that the best spectral location of the LSPR band for maximum enhancement is coincident with the laser excitation wavelength. In practice, this is often not the case as has been revealed by careful wavelength-dependence studies.[25] By measuring benzenethiol on planar substrates, it was concluded that the "enhancement of both fields occurs optimally when the frequencies of the incident and scattered fields straddle the LSPR extinction spectrum".[26] In other words, for maximum enhancement, the LSPR band should be red-shifted with respect to the excitation wavelength. In order to assess the impact the LSPR frequency on our SERS signal, we fixed the excitation wavelength at 785 nm while measuring a range of the previously synthesized nanostar suspensions.[10,27] Figure 4A shows SERS spectra acquired from solutions of 4-NTP adsorbed on gold nanostars. As shown previously, the series of suspensions contained gold nanostars of varying morphology and therefore possessed characteristically different LSPR bands. From Figure 4A, one can observe

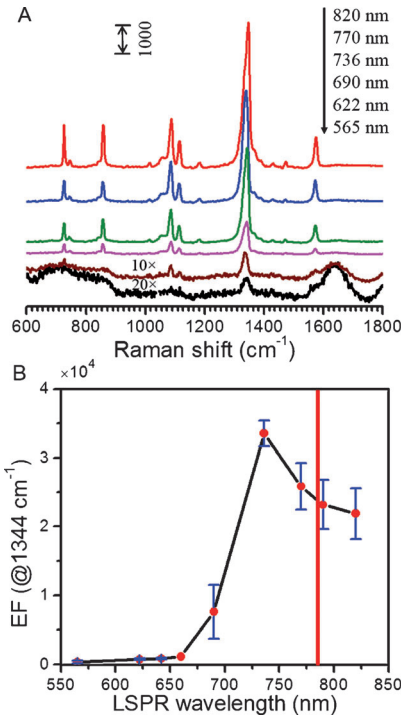

Figure 4. LSPR-dependent SERS enhancement. A) SERS spectra of 4-NTP in the presence of gold nanostars with LSPR bands of 565, 622, 690, 736, 770 and 820 nm, respectively. Note that the SERS spectra shown in (A) have been offset vertically for clarity. SERS spectra of 565 and 622 nm gold nanostars are 20 and 10 times magnified, respectively, for plotting purposes. B) SERS EFs as a function of the LSPR wavelength of gold nanostars. The red solid line shown in (B) indicates the 785 nm laser wavelength position.

that the SERS intensity is very weak when the LSPR bands for the nanostars are at 565 nm and 690 nm but it significantly increases as the LSPR band red-shifts to 736 nm. Surprisingly, within the range of measured nanostar suspensions, it seems that the maximum SERS EF can be achieved from the gold nanostar with the 736 nm LSPR band. To gain a direct understanding of this behavior, we plotted the SERS EFs as a function of the LSPR wavelength of gold nanostar (Figure 4B). The estimated SERS EF first increases and then decreases with increasing LSPR wavelength—with the optimal EF occurring at a wavelength *lower* than the laser excitation. That is, the optimal LSPR band (736 nm here) with maximum EF is blue-shifted from the NIR 785 nm excitation line. The SERS intensity dependence on the LSPR wavelength shows the similar trend as well (Figure S1).

Clearly, our finding is in sharp contrast to the observations of prior wavelength-dependence studies.[25,28] While such observations are in full agreement with theoretical predictions based on the EM mechanism, planar SERS substrates do not feature competitive extinction action, which is a hallmark of colloidal suspensions. On the other hand, our work has used the colloidal suspension of gold nanostar as the amplifying agent, which is equally relevant to most applications of in vitro and in vivo biological sensing and imaging. The validity of our results is evidenced by the very recent observations of an analogous effect in suspensions of gold nanorods and nanospheres.[29] Evidently, the antagonistic interplay between the optical extinction and the electromagnetic enhancement emanating from the same medium (nanostars) causes the LSPR band with maximum SERS EF to be off-resonant and, critically, to be blue-shifted from the incident excitation wavelength for suspensions of gold nanostars. This also underlines that the relationship between optical extinction and SERS enhancement is not as straightforward as previously anticipated thereby necessitating a specialized design and optimization strategy for the application and nanoprobe of interest. To the best of our knowledge, this also represents the first demonstration of the extinction-enhancement interplay in back-scattering (reflection) mode, which is the preferred mode of operation for most environmental and biosensing applications. The measurements in the back-scattering geometry shown in Figure 4 reflect a larger blue-shift of the LSPR band in relation to transmission geometry.

In summary, we have tailored the LSPR band of gold nanostars from the visible to the NIR region using the gold seed-mediated method to systematically investigate the effect of LSPR wavelength and concentration of nanostars on the SERS enhancement. We observe that the EF initially increases before steeply decreasing with the rising concentration of gold nanostars, the latter occurring as a direct consequence of the attenuation of the incident and Raman-scattered light in solution. Furthermore, we demonstrate that the maximum SERS EF in the nanostar colloidal suspension occurs at a LSPR band blue-shifted from the NIR 785 nm laser excitation wavelength. We conjecture that the gold nanostars not only enhance the effective Raman signal by virtue of the high density of hot spots, but also reduce the intensity of the light in propagation thereby hindering the overall SERS impact in the suspension as a function of the optical penetration path. Since gold nanostars ably support plasmon-assisted scattering of molecules and can be bioconjugated to a diverse set of ligands, this present work provides effective insight and guidelines for the synthesis and use of such nanoparticles and optimization of the optics design. Collectively, this study informs about the architecture and deployment of nanoprobes, which in concert with molecular targeting strategies, are being currently developed in our laboratory for early detection of breast cancer recurrence as distant metastasis and for speedy assessment of therapeutic benefit. Such nanoprobes offer a new route for a convenient, noninvasive, and repeatable "liquid biopsy" by providing a reliable template for assessing cell-free, circulating markers that reflect tumor burden.

Received: September 20, 2014
Published online: October 21, 2014

Keywords: nanoparticles · optical extinction · plasmonics · surface-enhanced Raman spectroscopy · suspension

[1] G. Wang, R. J. Lipert, M. Jain, S. Kaur, S. Chakraborty, M. P. Torres, S. K. Batra, R. E. Brand, M. D. Porter, *Anal. Chem.* **2011**, *83*, 2554 – 2561.
[2] J. Kneipp, B. Witting, H. Bohr, K. Kneipp, *Theor. Chem. Acc.* **2010**, *125*, 319 – 327.
[3] X. Qian, X. H. Peng, D. O. Ansari, Q. Yin-Goen, G. Z. Chen, D. M. Shin, L. Yang, A. N. Young, M. D. Wang, S. Nie, *Nat. Biotechnol.* **2008**, *26*, 83 – 90.
[4] K. Kneipp, H. Kneipp, I. Itzkan, R. R. Dasari, M. S. Feld, *Chem. Rev.* **1999**, *99*, 2957 – 2976.
[5] K. Kneipp, Y. Wang, H. Kneipp, L. T. Perelman, I. Itzkan, R. R. Dasari, M. S. Feld, *Phys. Rev. Lett.* **1997**, *78*, 1667.
[6] S. Nie, S. R. Emory, *Science* **1997**, *275*, 1102 – 1106.
[7] M. Li, S. K. Cushing, J. Zhang, S. Suri, R. Evans, W. P. Petros, L. F. Gibson, D. L. Ma, Y. X. Liu, N. Wu, *ACS Nano* **2013**, *7*, 4967 – 4976.
[8] S. R. Panikkanvalappil, M. A. Mackey, M. A. El-Sayed, *J. Am. Chem. Soc.* **2013**, *135*, 4815 – 4821.
[9] S. M. Morton, L. Jensen, *J. Am. Chem. Soc.* **2009**, *131*, 4090 – 4098.
[10] Y. Wang, B. Yan, L. Chen, *Chem. Rev.* **2012**, *113*, 1391 – 1428.
[11] A. K. Singh, S. A. Khan, Z. Fan, T. Demeritte, D. Senapati, R. Kanchanapally, P. C. Ray, *J. Am. Chem. Soc.* **2012**, *134*, 8662 – 8669.
[12] L. M. Liz-Marzán, *Langmuir* **2006**, *22*, 32 – 41.
[13] D. K. Lim, K. S. Jeon, J. H. Hwang, H. Kim, S. Kwon, Y. D. Suh, J. M. Nam, *Nat. Nanotechnol.* **2012**, *6*, 452 – 460.
[14] D. K. Lim, K. S. Jeon, H. M. Kim, J. M. Nam, Y. D. Suh, *Nat. Mater.* **2010**, *9*, 60 – 67.
[15] K. M. Mayer, J. H. Hafner, *Chem. Rev.* **2011**, *111*, 3828 – 3857.
[16] M. Li, S. K. Cushing, J. Zhang, J. Lankford, Z. P. Aguilar, D. Ma, N. Wu, *Nanotechnology* **2012**, *23*, 115501.
[17] Y. Zhang, J. D. Lin, V. Vijayaragavan, K. K. Bhakoo, T. T. Y. Tan, *Chem. Commun.* **2012**, *48*, 10322 – 10324.
[18] C. M. Hessel, M. R. Rasch, J. L. Hueso, B. W. Goodfellow, V. A. Akhavan, P. Puvanakrishnan, J. W. Tunnel, B. A. Korgel, *Small* **2010**, *6*, 2026 – 2034.
[19] M. Li, J. Zhang, S. Suri, L. J. Sooter, D. Ma, N. Wu, *Anal. Chem.* **2012**, *84*, 2837 – 2842.
[20] M. Li, S. K. Cushing, H. Liang, S. Suri, D. Ma, N. Wu, *Anal. Chem.* **2013**, *85*, 2072 – 2078.

[21] J. B. Jackson, S. L. Westcott, L. R. Hirsch, J. L. West, N. J. Halas, *Appl. Phys. Lett.* **2003**, *82*, 257 – 259.
[22] T. van Dijk, S. T. Sivapalan, B. M. DeVetter, T. K. Yang, M. V. Schulmerich, C. J. Murphy, R. Bhargava, P. S. Carney, *J. Phys. Chem. Lett.* **2013**, *4*, 1193 – 1196.
[23] Y. G. Zhou, N. V. Rees, R. G. Compton, *Chem. Commun.* **2012**, *48*, 2510 – 2512.
[24] M. A. Mahmoud, M. A. El-Sayed, *J. Phys. Chem. Lett.* **2013**, *4*, 1541 – 1545.
[25] A. D. McFarland, M. A. Young, J. A. Dieringer, R. P. Van Duyne, *J. Phys. Chem. B* **2005**, *109*, 11279 – 11285.
[26] P. L. Stiles, J. A. Dieringer, N. C. Shah, R. P. Van Duyne, *Annu. Rev. Anal. Chem.* **2008**, *1*, 601 – 626.
[27] S. L. Smitha, K. G. Gopchandran, T. R. Ravindran, V. S. Prasad, *Nanotechnology* **2011**, *22*, 265705.
[28] R. A. Alvarez-Puebla, D. J. Ross, G. A. Nazri, R. F. Aroca, *Langmuir* **2005**, *21*, 10504 – 10508.
[29] S. T. Sivapalan, B. M. DeVetter, T. K. Yang, T. van Dijk, M. V. Schulmerich, P. S. Carney, R. Bhargava, C. J. Murphy, *ACS Nano* **2013**, *7*, 2099 – 2105.

